Progress on an optical trapping assay to measure DNA folding pathways in sperm

Luka M. Devenica, Bishop Grimm, Terri-Anne Hultum, Ashley R. Carter*
Department of Physics, Amherst College, Amherst, MA, USA, 01002

ABSTRACT

DNA undergoes a dramatic condensation in sperm nuclei. During this condensation, the DNA rapidly folds into a series of toroids when protamine proteins replace histone proteins. Measuring the mechanics and folding pathway for this incredible condensation is an important goal. Here, we report on progress to use an *in vitro*, optical trapping assay to measure the DNA folding dynamics for this process. In this assay, a single DNA molecule with its associated histone proteins is attached to a cover slip and to an optically trapped bead. Movement of the optical trap applies a force on the bead, stretching the DNA to a particular extension. When protamine is added, the extension changes, allowing us to measure the preliminary folding dynamics for the process.

Keywords: Optical trap, optical tweezers, DNA folding, protamine, histone, single molecule, force spectroscopy

1. INTRODUCTION

DNA inside sperm nuclei is 40 times more compact than the DNA inside somatic nuclei.[1] This is necessary to create a hydrodynamic sperm capable of efficient transport[2] and is crucial in protecting the DNA from UV damage.[3, 4] To compact the DNA to these near crystalline levels, the sperm alters how the DNA is folded, replacing the histone proteins that fold the DNA in somatic cells with protamines.[2, 5] Protamines are small globular proteins (~50 amino acids long) that are rich in positively charged residues like arginine. To fold the DNA, protamines bind to the major groove of DNA[2] and loop it into a toroid with an approximate diameter of 50 nm.[6-9] Multiple toroids then stack within the nucleus,[3] creating a compact sperm head. While previous studies have looked at DNA folding by either histones[10-13] or protamines,[6, 8, 9] our goal is to study the DNA folding pathway for histone replacement by protamine.

A powerful method to examine DNA folding is single-molecule force spectroscopy using optical trapping.[10, 14-22] In one type of optical trapping experiment (Figure 1), a micron-sized, polystyrene bead is trapped by a focused laser *in vitro* and is tethered to the sample surface by a single DNA molecule. Specifically, the DNA is biochemically linked to the bead at one end and to the surface of the microscope cover slip at the other end. If the optical trap is moved relative to the surface, then the bead moves with the trap, creating a stretching force F on the DNA tether that unfolds it to a particular extension x. Measurements of force and extension can then be used to determine the kinetic and thermodynamic properties of the different wrapping or looping states in the DNA folding pathway.[23]

Here we report on progress to create this optical trapping experiment. We first constructed an optical trapping system capable of single-molecule force spectroscopy using published protocols.[24-28] The system (Figure 2) consists of an optical trap formed by a 1064-nm-wavelength, crystal laser, which is directed into a microscope objective, and a 945-nm-wavelength diode laser that is used for detection. Once the system was constructed, we measured stable trapping of up to 15 μm into solution as well as bead detection signals with <1 nm resolution. Finally, we created a series of programs to take force spectroscopy measurements in LabView, including programs to measure force and extension.

This assay should now be capable of measuring DNA folding dynamics during histone replacement by protamine. Measurement of these dynamics is important in studies of fertility, biomaterials, and single molecule biophysics.

*acarter@amherst.edu; phone: 1 413 542-2593; fax: 1 413 542-5821; webpage: carterlaboratory.com

2. METHODS

2.1 DNA preparation

DNA for the single molecule assay was generated by using polymerase chain reaction (PCR) using published methods.[27] Briefly, we purchased DNA primers (Integrated DNA Technologies) that amplified a 794 nm (2335 bp) region of λ-phage DNA (New England Biolabs). One DNA primer contained a 5′- biotin and the other had a 3'- digoxigenin. PCR with these primers produced DNA that could be anchored to a streptavidin-coated bead at one end and to an anitdigoxigenin-coated cover slip at the other end. DNA was gel purified using a gel extraction kit (Qiagen) and a spectrophotometer (NanoDrop One, Thermo Fisher) was used to measure the DNA concentration.

2.2 Sample preparation

To prepare the sample, we first constructed sample chambers from a microscope slide, double-sided sticky tape, five-minute epoxy, and a microscope cover slip. The tape was used as a spacer between the slide and cover slip to create a chamber with ~15 μL of volume and openings at both ends to allow for buffer flow. The addition of epoxy was required to keep the chamber intact as the tape would often get waterlogged.

After constructing the sample chamber, we prepared the biological assay. This assay (Figure 1) consisted of a 560-nm-diameter, streptavidin-coated, polystyrene bead (Spherotech) tethered to the sample surface by a single DNA molecule.[27] To prepare this assay, we added 60 μL of 560-nm-diameter, streptavidin-coated, polysterene beads (1 % w/v, 170 pM, Spherotech) to 200 μL of Phos-Tween [100 mM NaPhos (pH = 7.4) and 0.4% Tween-20 (Bio-Rad)] and centrifuged the solution with a microcentrifuge at 10,000 rpm for 2 min. After removing the supernatant, we repeated the process two more times. This coats unbound regions of the beads with phosphate and prevents bead sticking. Beads were then reconstituted in 30 μL of wash buffer (WB). WB was made by combining 25 mM Tris-HCl (pH = 7.5), 1 mM dithiothreitol, 1 mM sodium chloride, 1 mM magnesium acetate, 3 mg/ml bovine serum albumin (concentration cited is that before filtration through a 0.2-μm filter), and 0.4% Tween-20. Beads were sonicated in a cup sonicator (Qsonica) until they were monodispersed. These monodispersed beads were then incubated in a test tube at room temperature with 30 μL of 200 pM DNA for 1 hour. The ~2:1 ratio of beads to DNA led to a greater probability of beads only attaching to one DNA molecule. Concurrent to bead-DNA preparation, we flowed on a solution of 20 μg/mL antidigoxigenin (Roche, from Sheep) into the flow chamber and incubated the solution for 1 hour at room temperature to allow the antidigoxigenin to nonspecifically adhere to the cover slip surface. The antidigoxigenin solution was dissolved in 100 mM NaPhos. After incubation, we rinsed the flow chamber with 400 μL of WB, waited 10 minutes, and rinsed with 400 μL of WB again. This removed unbound protein. We then added the bead-DNA solution to the flow chamber and let it incubate for 1 h at room temperature. The unbound bead-DNA complexes were removed by a final rinse with 400 μL of WB.

To make sample chambers with beads stuck to the surface, we first flowed through 20 μL of 1 pM bead solution [either 510-nm-diameter or 560-nm-diameter, streptavidin-coated polystyrene beads (Spherotech) diluted in deionized water] in to the sample chamber. Then, we flowed 20 μL of 100 mM magnesium acetate and waited 2 minutes before rinsing with 200 μL of deionized water.

2.3 Optical trapping instrument

For this study, we used an optical-trapping instrument (Figure 2) modeled after previous work.[24-29] To create the optical trap, we coupled a high-powered crystal laser (Nd:YVO_4; λ = 1064 nm, ~500 mW at the focus) into a microscope (Eclipse Ti-U, Nikon, with 1.4 NA oil 100X objective). The crystal laser produces a TEM00 mode with a Gaussian intensity profile along with other non-spherically symmetric modes. To filter out these modes, we used a single-mode, polarization-maintaining, optical fiber (Thorlabs) that spatially filtered the beam at the cost of some added intensity noise. In the future, intensity noise could be removed with an intensity stabilization system featuring an acousto-optic modulator.[27] A fiber port (KT110, Thorlabs) at the exit of the fiber contained two lenses (focal lengths of 6 mm and 75 mm) that set the beam diameter (5 mm) and the collimation of the beam. Movement of the fiber output relative to the lenses changed the collimation and therefore the axial location of the trap focus relative to the sample plane in the microscope. The combination of a half-wave plate and polarizing beam splitter allowed for manual selection of the trap intensity. To translate the focus of the trap laser in the microscope, we placed a mirror on a gimbal mount in a confocal plane to the

back aperture of the objective. Pure rotations of the mirror using the gimbal mount in this plane would then turn into pure translations in the sample plane.[24] Electronic movement of the mirror was achieved by adding a piezo stack (S-330, Physik Instrumente, 20 nrad resolution). To create the confocal plane for the mirror mount we used a telescope system (focal lengths of 250 mm and 400 mm) that also increased the beam diameter to 8.0 mm. The alignment of the laser to the microscope objective was done by setting the fiber port at the exit of the fiber on a 3D stage and by adding a periscope system (two mirrors) before the gimbal-mounted mirror. The presence of both of these systems allowed for quick alignment of the beam.

In order to detect the bead, we used the back scattered light of a separate diode laser (Lumics, λ = 945 nm, ~2 mW at the laser focus) for detection.[30] The optics for coupling this detection laser into the microscope were the same as the optics for the trap laser, except for two important differences. The first difference was the presence of a dichroic mirror (1000 nm high-pass, Semrock) in the path of the detection laser that reflected the detection laser on to the beam path of the trap laser. The second difference was a quarter-wave plate, which acted in conjunction with the polarizing beam splitter to select out the back scattered signal. Specifically, the quarter-wave plate changes the detection light out of the laser from linearly polarized to circularly polarized, and it changes the back-scattered light from the microscope from circularly polarized to linearly polarized. However, since the back-scattered light has an added 180° phase shift, the polarization of the back-scattered light is opposite from the original laser light, allowing for separation by the polarizing beam splitter. Detection of this back-scattered light was done with a rotatable, quadrant photodiode (PDQ80A, Thorlabs) on a 2D stage. An iris in front of the quadrant photodiode selected the back-scattered light.[28]

2.4 Data collection and processing

Data collection consisted of measuring the back-scattered signal from the trapped bead using the quadrant photodiode. The quadrant photodiode output four voltages: V_1 (upper right), V_2 (lower right), V_3 (upper left), and V_4 (lower left). A custom electronics box then calculated the signals in x ($[V_1 + V_2 - V_3 - V_4]/[V_1 + V_2 + V_3 + V_4]$), y ($[V_1 + V_2 - V_3 - V_4]/[V_1 + V_2 + V_3 + V_4]$), and z ($V_1 + V_2 + V_3 + V_4$) and added a tunable offset to these voltages to remove background. These voltage outputs were then differentially amplified (1000x) and run through an anti-aliasing filter with a variable corner frequency of 0-100 kHz (USBPGF-S1, Alligator Electronics) before being digitized by a data acquisition card (BNC-2090A, National Instruments, 16 bit, 20 V range).

The raw x, y, and z signals from the quadrant photodiode were transformed into measurements using a series of software programs (Figure 3) written in LabVIEW (National Instruments). First, we used a coarse alignment program to move the piezo stage (P-733 stage with E-712 controller, Physik Instrumente) until a bead tethered to the surface was trapped in the optical trap. Second, a height adjust program then determined the vertical location of the trapped bead above the surface by monitoring the z signal of the quadrant photodiode as the stage brought the sample into contact with the trapped bead. When the trapped bead contacted the sample, the bead moved out of the trap, changing the z signal. We found this location and then lowered the stage 200 nm, setting the trap height z_{trap} to the radius of the bead, r_b, plus 200 nm. Third, a positional calibration program then calibrated the x and y signals output by the quadrant photodiode into positional measurements of the bead (x_{bd} and y_{bd}, respectively) in nanometers. Specifically, we moved the detection laser through the trapped bead in both x and y using the piezo mirror and monitored the voltage signal output by the quadrant photodiode. A fit to the data established the calibration factor for changing voltage on the quadrant photodiode into nanometers. Movements of the piezo mirror in nanometers are known through earlier calibrations that use a stuck bead on the stage to determine the location of the detection laser before and after a change in voltage output to the mirror. Next, a DNA stretching program found the location of where the DNA was tethered to the surface (the tether point) and centered the trap above this location. To do this, the stage was moved back and forth in either x or y, stretching the DNA and causing the bead to move out of the trap. The program then plotted the bead position as a function of stage movement and calculated the force-extension curve. The place where the Brownian motion of the bead is the highest and the extension and force are zero is the location of the tether point. Lateral movement of the stage (x_{stage} or y_{stage}) is then measured from this tether point. After centering the trap above the tether point, all of the programs were repeated for accuracy.

For force spectroscopy measurements or to find the tether point, the force on the DNA F and the extension of the DNA x need to be determined from measurements of x_{bd} and x_{stage}. This determination is given by the trapping geometry (Figure 1).[21] Briefly, we calculated the axial bead location, z_{bd}, using the equation,

$$z_{\mathrm{bd}} = \frac{z_{\mathrm{trap}}}{\left(\frac{k_{\mathrm{z}}}{k_{\mathrm{x}}}\right)\left(\frac{x_{\mathrm{stage}} - x_{\mathrm{bd}}}{x_{\mathrm{bd}}}\right) + 1}. \quad (1)$$

Here the ratio of the axial and lateral trap stiffnesses (k_z and k_x, respectively) is determined beforehand by measuring the Brownian motion of the bead in both x and z using the equipartition method.[26] Other methods are used to make sure this trap stiffness is robust.[26] Determining z_{bd} allows for the calculation of the extension x using the property of similar triangles,

$$x = \frac{z_{\mathrm{trap}} - z_{\mathrm{bd}}}{\sin^{-1}\left[\tan^{-1}\left(\frac{z_{\mathrm{trap}} - z_{\mathrm{bd}}}{x_{\mathrm{stage}} - x_{\mathrm{bd}}}\right)\right]} - r_{\mathrm{bd}}. \quad (2)$$

The force exerted on the DNA has a similar calculation and is,

$$F = \frac{k_{\mathrm{x}} x_{\mathrm{bd}}}{\cos^{-1}\left[\tan^{-1}\left(\frac{z_{\mathrm{trap}} - z_{\mathrm{bd}}}{x_{\mathrm{stage}} - x_{\mathrm{bd}}}\right)\right]}. \quad (3)$$

Once the force and extension are determined, force spectroscopy measurements on single DNA molecules are possible.

Force-extension curves are fit with a modified worm-like chain model to determine the DNA contour length, L, or the persistence length, p. In the worm-like chain model,[31] DNA is modeled as a semi-flexible polymer with a stretching force, which depends on the DNA extension, the thermal energy, $k_B T$, the contour length of the DNA, and the persistence length,

$$F = \frac{k_{\mathrm{B}} T}{p}\left(\frac{1}{4\left(1 - \frac{x}{L}\right)^2} - \frac{1}{4} + \frac{x}{L}\right). \quad (4)$$

To apply this fit, we use a corrected version[32] of the interpolation formula[33] to this model, which is useful when fitting experimental data.

3. RESULTS AND DISCUSSION

3.1 Stability of optical trap

To get a quick measurement of the trapping capability of our system, we trapped a 560-nm-diameter polystyrene bead in the 1064-nm-wavelength laser at a trap height z_{trap} of 500 nm. We then moved the focusing knob of the objective to translate the z position of the laser further into solution (Figure 4). Eventually, the bead fell out of the trap, and we recorded this location using the micrometer markings on the objective focus knob. We achieved stable trapping to at least 15 ± 1 μm for all trials (N=5). This is much greater than the ~1 μm depth needed for the DNA folding assay.

3.2 Detection signal sensitivity

To measure the capability of the detection system for our instrument (Figure 5), we translated a 510-nm-diameter polystyrene bead stuck to the cover slip surface through the detector laser and measured the quadrant photodiode signal in x, y, and z. We then fit a line to each of the central regions of the signal to measure a sensitivity in V/nm. Without amplification, the sensitivity in x, y, and z was 0.4 ± 0.1 mV/nm, 0.9 ± 0.1 mV/nm, and 0.3 ± 0.1 mV/nm, respectively. This is just at the bit noise of our 16 bit data acquisition card with the 20 V range ($20/2^{16}$ = 0.3 mV). Thus, even without amplification we have enough signal to measure 1 nm movements. Adding 1000X amplification to this signal, increases the sensitivities by 1000 and allows for measurements of <1 nm. Since DNA folding by histones creates nucleosomes that contain ~70 nm (~200 bp) of DNA,[11-13] while DNA folding by protamines creates loops that contain ~150 nm (~440 bp) of DNA.[6-9] The <1 nm resolution of the assay should be sufficient for measuring these changes.

3.3 Future force spectroscopy measurements

To perform force spectroscopy measurements with this assay requires measuring force and extension. Here we have programmed software to measure force-extension curves (Figure 3) and can also hold the force on the DNA constant (in a force clamp mode)[23, 26] while measuring the extension.

We now need to perform these measurements on DNA tethers that are folded by either histones or protamine. Some interesting experiments would be to vary the ionic strength of the solution, protamine or histone concentration, DNA length, protein composition, or DNA sequence and observe the effects of these parameters on the folding pathway. Completing these measurements would give insight into the thermodynamic or kinetic parameters of the histone replacement pathway, which is important in studies of fertility, biomaterials, and single molecule biophysics.

Acknowledgments

We would like to thank Jim Kubasek for custom machining and Brian Crepeau for custom electronics. This work was supported by a Cottrell Science Award from the Research Corporation (ARC, Award #23239), a CAREER award from the National Science Foundation (ARC, Project #1653501), and Amherst College.

FIGURES

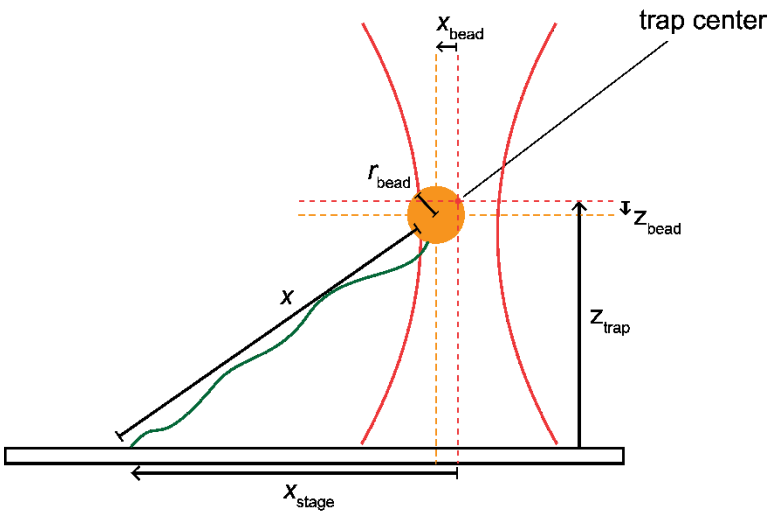

Figure 1. Geometry of the single molecule optical trapping assay. A bead (*orange*) with radius r_{bd} is attached to the surface by a DNA molecule (*green*) and trapped by a focused laser (*red lines*). Movement of the stage, x_{stage}, applies a force to the DNA stretching it to an extension, x. This causes the bead to move out of the trap center by an amount x_{bd} and z_{bd}. The trap center is set to a distance z_{trap} above the surface.

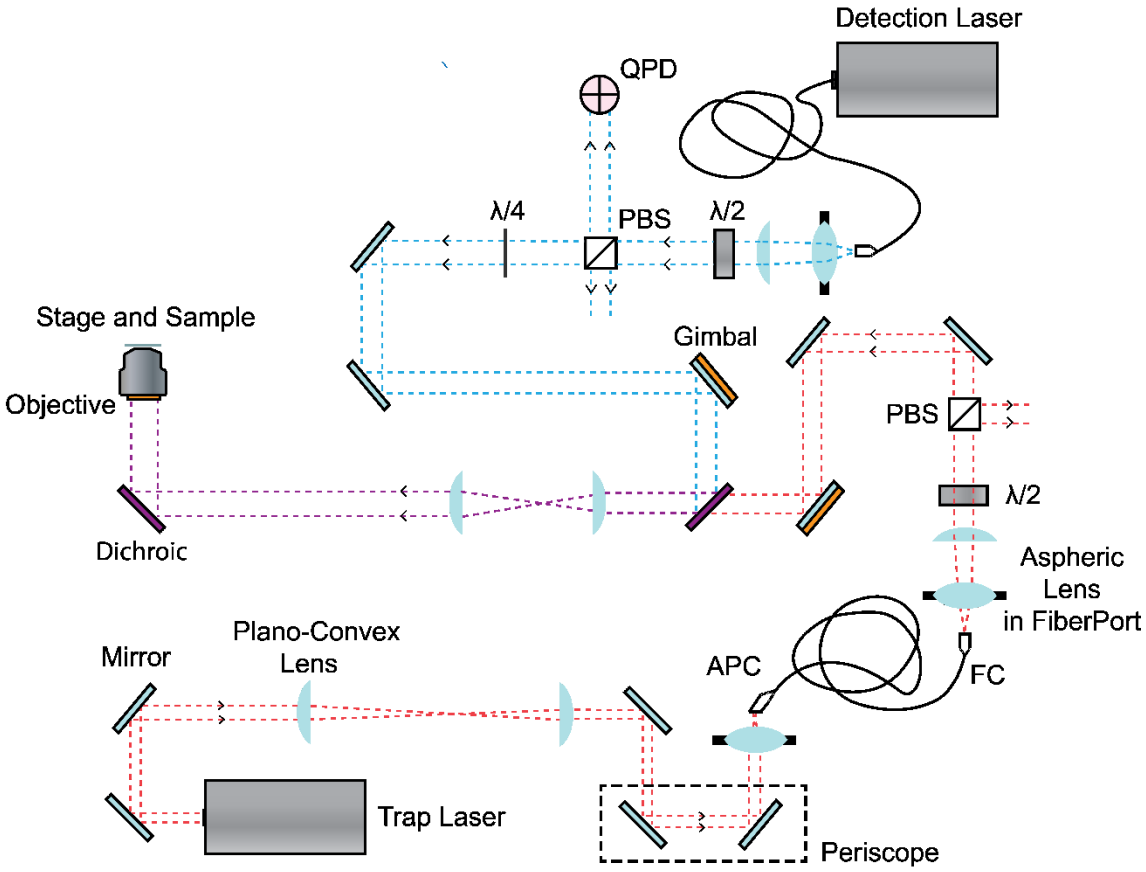

Figure 2. Diagram of the optical trapping system. There are two lasers: the 1064-nm-wavelength trap laser (*red dashed lines*) and the 945-nm-wavelength detection laser (*blue dashed lines*). The trap laser first passes through a periscope (two mirrors), which consists of two mirrors (*light blue*). This allows for alignment into the telescope, which sizes the beam for coupling into the angled physical contact (APC) end of an optical fiber. A second periscope aligns the beam into the 3-axis fiber port with aspheric lens. The trap laser exits the fiber at the flat contact (FC) end and is now spatially filtered. The aspheric lens in the fiber port and the subsequent lens are used to collimate the beam at the fiber exit. The trap laser is then attenuated with a half-wave plate (λ/2) and a polarizing beam splitter (PBS). The fiber-coupled diode laser follows a similar path and is set to the same diameter as the trap laser (5-mm-diameter). Both beams then have a periscope after the PBS which allows for quick alignment into the microscope, and both have a gimbal-mounted mirror, which translates the beam in the sample plane. This gimbal-mounted mirror lies in a conjugate plane (*orange*) with the back-aperture of the objective, so that pure rotations of the mirror create pure translations of the laser in the sample plane. The dichroic mirror (*purple*) couples the two beams on to the same beam path. The telescope after the dichroic mirror expands the beam by a factor of two and creates the conjugate plane at the gimbal-mounted mirror. A second dichroic below the objective couples in the imaging light (*not shown*) on to the beam path. The objective focuses the two lasers in the sample plane. The detection laser scatters off the bead in the sample plane, and the quarter-wave plate (λ/4) in the detection laser path isolates this back-scattered signal on the quadrant photodiode (QPD). Diagram not to scale.

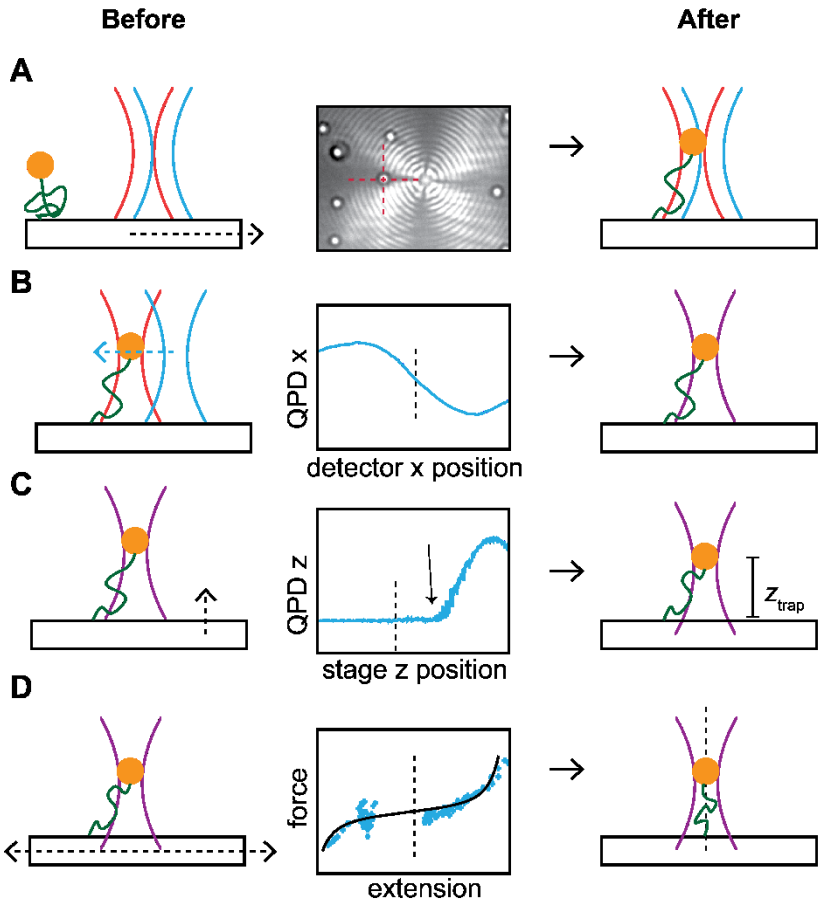

Figure 3. Measurement procedure. **A**) First, a bead tethered to the surface is optically trapped. To do this, we view the sample plane with a camera and move the stage with the bead (*red dashed lines*) to the optical trap (*bright spot*). **B**) Second, the detection laser is aligned. The detection laser (*blue*) is translated through the trapped bead using the piezo-controlled, gimbal-mounted mirror. The lateral signal on the QPD (*e.g.* QPD x) is recorded as the detector moves. The laser is then moved to the center of the signal (*black dashed line*) to align the beam. **C**) Third, the height above the surface is set. The stage is moved toward the trapped bead while recording the axial signal on the QPD (QPD z). This signal begins to change when the stage first hits the bead (*arrow*) and moves it out of the trap. We set z_{trap} to be a desired amount (*black dashed line*) from this location. **D**) Finally, we find the location of the tether point. The stage is moved laterally in both directions while the lateral bead position is recorded. This allows for measurement of the force-extension curve. Fitting of the curve to a modified worm-like chain model (*black line*) allows for determination of the tether point (*black dashed line*).

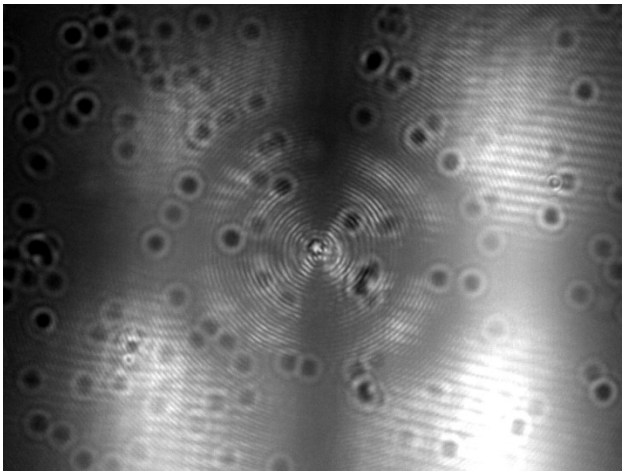

Figure 4. Image of a bead trapped in the focus of the 1064-nm-wavelength laser. Beads stuck to the surface (*black*) are out of focus and are located several microns below.

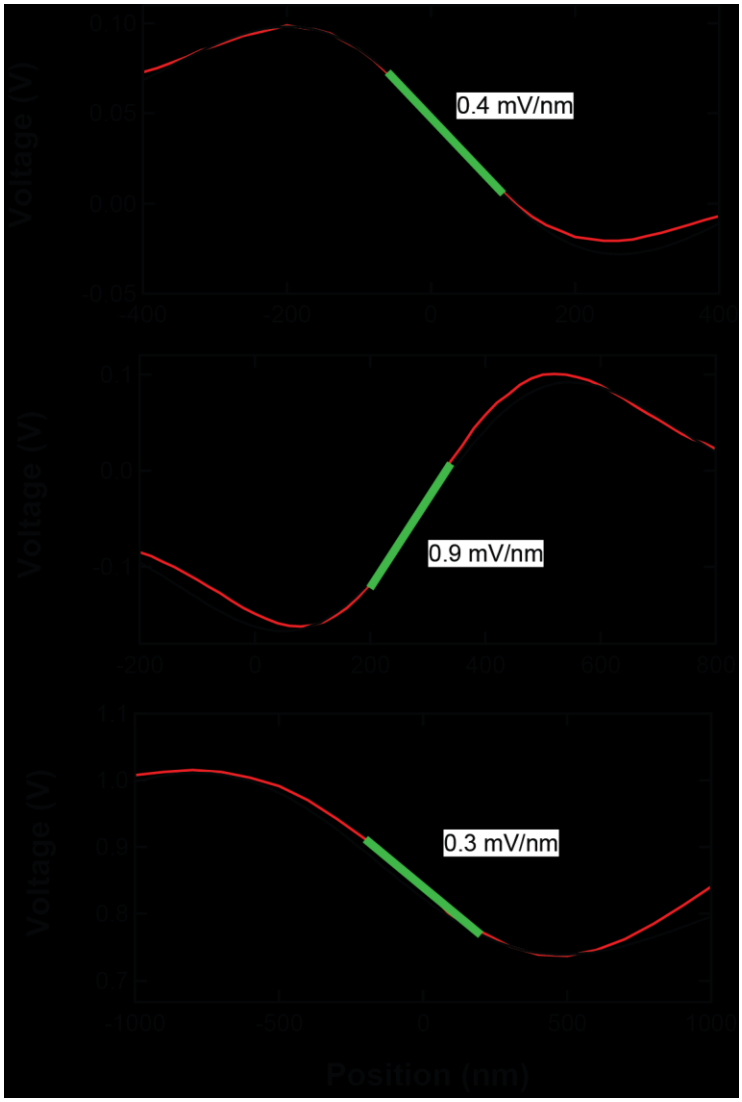

Figure 5. QPD signals of a 510-nm-diameter bead in *x*, *y*, and *z*. The average voltage on the QPD is recorded as the sample with the attached stuck bead is translated in 20 nm increments. Measurements of this voltage with bead position (*red*) can be fit by a derivative of a Gaussian (*black*).[34] A line (*green*) is fit to the central region, and the slope determines the sensitivity in V/nm.

REFERENCES

[1] N. V. Hud, F. P. Milanovich, and R. Balhorn, "Evidence of novel secondary structure in DNA-bound protamine is revealed by Raman spectroscopy," Biochemistry, 33(24), 7528-7535 (1994).

[2] R. Balhorn, "The protamine family of sperm nuclear proteins," Genome Biol, 8, (2007).

[3] W. S. Ward, "Function of sperm chromatin structural elements in fertilization and development," Mol Hum Reprod, 16(1), 30-6 (2010).

[4] S. Gonzalez-Rojo, C. Fernandez-Diez, S. M. Guerra *et al.*, "Differential Gene Susceptibility to Sperm DNA Damage: Analysis of Developmental Key Genes in Trout," PLOS ONE, 1-21 (2014).

[5] D. Poccia, "Remodeling of nucleoproteins during gametogenesis, fertilization, and early development," International review of cytology, 105, 1-65 (1986).

[6] R. Balhorn, L. Brewer, and M. Corzett, "DNA condensation by protamine and arginine-rich peptides: analysis of toroid stability using single DNA molecules," Mol Reprod Dev, 56(2 Suppl), 230-4 (2000).

[7] L. Brewer, M. Corzett, and R. Balhorn, "Condensation of DNA by Spermatid Basic Nuclear Proteins," Journal of Biological Chemistry, 277(41), 38895-38900 (2002).

[8] L. R. Brewer, M. Corzett, and R. Balhorn, "Protamine-induced condensation and decondensation of the same DNA molecule," Science, 286(5437), 120-3 (1999).

[9] L. H. Cree, R. Balhorn, and L. R. Brewer, "Single molecule studies of DNA-protamine interactions," Protein Pept Lett, 18(8), 802-10 (2011).

[10] M. L. Bennink, S. H. Leuba, G. H. Leno *et al.*, "Unfolding individual nucleosomes by stretching single chromatin fibers with optical tweezers," Nature Structural Biology, 8(7), 606-610 (2001).

[11] F. T. Chien, and J. van Noort, "10 years of tension on chromatin: results from single molecule force spectroscopy," Curr Pharm Biotechnol, 10(5), 474-85 (2009).

[12] S. Mihardja, A. J. Spakowitz, Y. Zhang *et al.*, "Effect of force on mononucleosomal dynamics," Proceedings of the National Academy of Sciences, 103(43), 15871-15876 (2006).

[13] B. D. Brower-Toland, C. L. Smith, R. C. Yeh *et al.*, "Mechanical disruption of individual nucleosomes reveals a reversible multistage release of DNA," Proceedings of the National Academy of Sciences of the United States of America, 99(4), 1960-1965 (2002).

[14] A. A. Almaqwashi, T. Paramanathan, I. Rouzina *et al.*, "Mechanisms of small molecule-DNA interactions probed by single-molecule force spectroscopy," Nucleic Acids Research, 44(9), 3971-3988 (2016).

[15] M. L. Bennink, L. H. Pope, S. H. Leuba *et al.*, "Single chromatin fibre assembly using optical tweezers," Single Molecules, 2(2), 91-97 (2001).

[16] U. Bockelmann, P. Thomen, B. Essevaz-Roulet *et al.*, "Unzipping DNA with optical tweezers: high sequence sensitivity and force flips," Biophysical Journal, 82(3), 1537-1553 (2002).

[17] C. Bustamante, S. B. Smith, J. Liphardt *et al.*, "Single-molecule studies of DNA mechanics," Curr Opin Struct Biol, 10(3), 279-85 (2000).

[18] D. N. Fuller, D. M. Raymer, J. P. Rickgauer *et al.*, "Measurements of single DNA molecule packaging dynamics in bacteriophage λ reveal high forces, high motor processivity, and capsid transformations," Journal of Molecular Biology, 373(5), 1113-1122 (2007).

[19] F. Kilchherr, C. Wachauf, B. Pelz *et al.*, "Single-molecule dissection of stacking forces in DNA," Science, 353(6304), (2016).

[20] K. Sakata-Sogawa, M. Kurachi, K. Sogawa *et al.*, "Direct measurement of DNA molecular length in solution using optical tweezers: detection of looping due to binding protein interactions," European biophysics journal, 27(1), 55-61 (1998).

[21] M. D. Wang, H. Yin, R. Landick *et al.*, "Stretching DNA with optical tweezers," Biophysical Journal, 72(3), 1335-1346 (1997).

[22] A. D. Smith, O. A. Ukogu, L. M. Devenica *et al.*, "Optical methods for measuring DNA folding," Modern Physics Letters B, 31(7), 37 (2017).

[23] M. T. Woodside, and S. M. Block, "Reconstructing folding energy landscapes by single-molecule force spectroscopy," Annu Rev Biophys, 43, 19-39 (2014).

[24] W. M. Lee, P. J. Reece, R. F. Marchington *et al.*, "Construction and calibration of an optical trap on a fluorescence optical microscope," Nat. Protocols, 2(12), 3226-3238 (2007).

[25] S. R. Okoniewski, A. R. Carter, and T. T. Perkins, "A Surface-Coupled Optical Trap with 1-bp Precision via Active Stabilization," Methods Mol Biol, 1486, 77-107 (2017).

[26] K. C. Neuman, and S. M. Block, "Optical trapping," Review of Scientific Instruments, 75(9), 2787-2809 (2004).

[27] A. R. Carter, Y. Seol, and T. T. Perkins, "Precision Surface-Coupled Optical-Trapping Assay with One-Basepair Resolution," Biophysical Journal, 96(7), 2926-2934 (2009).

[28] F. B. Shipley, and A. R. Carter, "Back-scattered detection yields viable signals in many conditions," Opt Express, 20(9), 9581-90 (2012).

[29] A. R. Carter, G. M. King, T. A. Ulrich *et al.*, "Stabilization of an optical microscope to 0.1 nm in three dimensions," Appl Opt, 46(3), 421-7 (2007).

[30] A. R. Carter, G. M. King, and T. T. Perkins, "Back-scattered detection provides atomic-scale localization precision, stability, and registration in 3D," Opt Express, 15(20), 13434-45 (2007).
[31] J. F. Marko, and E. D. Siggia, "Stretching DNA," Macromolecules, 28(26), 8759-8770 (1995).
[32] C. Bouchiat, M. D. Wang, J. F. Allemand *et al.*, "Estimating the Persistence Length of a Worm-Like Chain Molecule from Force-Extension Measurements," Biophysical Journal, 76(1), 409-413 (1999).
[33] C. Bustamante, J. F. Marko, E. D. Siggia *et al.*, "Entropic elasticity of lambda-phage DNA," Science, 265(5178), 1599-600 (1994).
[34] A. Pralle, M. Prummer, E. L. Florin *et al.*, "Three-dimensional high-resolution particle tracking for optical tweezers by forward scattered light," Microsc Res Tech, 44(5), 378-86 (1999).